Journal of Advanced Research in Numerical Heat Transfer

Journal homepage:
https://semarakilmu.com.my/journals/index.php/arnht/index
ISSN: 2735-0142

# Numerical Analysis for Enhanced Water Desalination in Solar Stills with Optimized Glass Cover Angles

Ayad Atiyah[1], Yaser Alaiwi[1], Mohammed Hussein Radhi[2] , Ahmad Jundi[1,*]

[1] Department of Mechanical Engineering, Altinbas University, Istanbul 34217, Turkey
[2] Department of Technology Engineering, Ashur University, Baghdad 10011, Iraq

**ARTICLE INFO**

***Article history:***
Received 19 April 2024
Received in revised form 18 May 2024
Accepted 19 June 2024
Available online 30 July 2024

***Keywords:***
Solar still; Thermal analysis; Numerical analysis; Algorithms; Optimizing

**ABSTRACT**

Water scarcity is a growing global issue that necessitates improved desalination techniques. This study aims to enhance solar still efficiency for water desalination in Baghdad's climate conditions. The research focuses on identifying the optimal glass cover tilt angle to maximize water production in single-slope solar stills. A multi-software approach was implemented, using SOLIDWORKS for design, ANSYS CFD for simulations, and MATLAB for numerical analysis. The solar still's performance was tested on July 25, 2023, from 9 AM to 5 PM, with tilt angles between 25° and 40°. Results show that a 25° angle is most effective, increasing water output by 3.3% compared to other angles. This optimal angle enhances solar radiation absorption while maintaining efficient condensation. Temperature distributions and evaporation rates were also analyzed to support these findings. These results provide valuable insights for optimizing solar still designs in regions with climate conditions similar to Baghdad, contributing to the development of more efficient water desalination technologies for water-scarce areas.

## 1. Introduction

Water, covering 70% of the Earth's surface, presents a paradox of abundance and scarcity, with only 0.5% accessible as freshwater. This scarcity, exacerbated by rapid population growth and pollution, poses severe challenges, currently affecting nearly 40% of the global population and projected to exceed 60% by 2025 [1,2]. Historical advancements in desalination, particularly since the early 1800s, have marked significant progress in water purification techniques. During this period, basic stills on ships evolved into more efficient systems, driven by the sugar industry's demand for evaporation technologies. This evolution led to the formal establishment of the desalination industry by the early 20th century, which has since experienced remarkable growth and technological advancements [1]. The principle of distillation relies on the thermodynamic property that the vapor produced from a boiling liquid mixture is enriched in the lower boiling components. This allows the separation of the liquid mixture into fractions with different compositions or even into its individual

* *Corresponding author.*
*E-mail address: ahmad.t.jundi@gmail.com (Ahmad Jundi)*

https://doi.org/10.37934/arnht.22.1.3145

components. The most basic distillation methods include batch distillation using simple distillation or continuous distillation using flash distillation [3]. Steam distillation is used for heat-sensitive materials, where introducing steam reduces the boiling point, thus preserving the integrity of these materials [4]. Solar distillation utilizes solar power to evaporate and condense water, emulating the natural hydrological cycle to purify water [5]. Each method represents significant technological advancements in the field of water purification.

The previous studies related to the research addressed several core aspects; the researchers in the study [6] modelled and simulated a hybrid cooling system for photovoltaic thermal cells using ANSYS Fluent, and the results showed a 15-20% drop in cell temperature when passing water behind them. Also, the researchers in the study [7] modelled an inclined integrated solar still with photovoltaic cells and a finned condenser unit and studied the effect of varying solar radiation and ambient temperature, finding that adding fins to the unit improved the distillation rate. Additionally, a study [8] tested a thermal model of a novel solar desalination system with parabolic trough mirrors, evaluating its performance under different weather conditions, indicating a 70% increase in summer productivity when using sun tracking. Study [9] focused on using integrated thermal photovoltaic solar stills, with the research achieving good agreement between theoretical and experimental performance values, attaining a thermal efficiency of 69.06%. Additionally, a study [10] reviewed various existing solar still designs, highlighting that passive stills are inexpensive but have lower efficiency. It concludes that further research into solar still parameters is needed to ensure cost-effectiveness and sustainability. In a previous study [11], the impact of glass cover thickness on solar still performance was investigated under winter conditions in Mehsana, India. The study utilized the Dunkle model to compare heat transfer coefficients and examined the effect of different glass cover thicknesses. The results showed that lower glass cover thickness leads to increased distillate output, with 4 mm being the optimal thickness for best performance. The findings highlight the importance of selecting appropriate glass thickness to enhance solar still productivity, especially in colder seasons and locations. In another study [12], a numerical analysis investigated the performance of a double-glass cover basin-type solar still compared to a conventional single-cover still under winter conditions. Based on energy balance equations, the mathematical model was solved using the Gauss-Seidel method. The results demonstrated that the double-glass cover configuration consistently outperformed the conventional still in terms of daily production, overall efficiency, and internal efficiency, with the performance gap widening at higher solar radiation levels. The study highlights the potential of double glass covers for enhancing solar still productivity and efficiency, especially under challenging winter conditions. A past study [13], conducted an experimental investigation of an inclined wick solar still operating under drop-by-drop conditions in Honda's region, Algeria. The study compared the performance of the inclined wick solar still with different wick thicknesses (thick, medium, and thin) to a conventional solar still. The experiments were carried out during clear days in April. The results showed that the inclined solar still with a thin wick achieved the highest daily production of 4.14 litre/m2.day and an efficiency of 46.66%, demonstrating an improvement of 23.21% and 12.56% respectively compared to the conventional solar still. The study also found that the cost per liter of distilled water was lowest for the inclined solar still with a thin wick at 0.011$/l, with a payback period of 77 days. The improved performance of the inclined wick solar still was attributed to several factors, including the use of a drop-by-drop feed system, elimination of side wall shadows, optimized inclination angle, reduced gap between evaporation and condensation surfaces, and the capillary effect of the wick material. The study highlights the potential of inclined wick solar stills for enhanced water desalination in arid and semi-arid regions.

While previous studies have made significant contributions to the field of solar desalination, several research gaps remain. One major gap is the limited use of precise numerical analysis tools

like MATLAB. Many studies have relied on experimental setups or simpler modelling techniques that may not capture the full complexity of the heat transfer and fluid dynamics involved in solar stills. Additionally, there is a scarcity of research that integrates multiple software platforms for a comprehensive analysis. Most studies focus on a single aspect of solar still design or use only one type of simulation software, which can limit the accuracy and robustness of the findings. For instance, combining SOLIDWORKS for design, ANSYS for CFD simulations, and MATLAB for numerical analysis can provide a more holistic and precise evaluation of solar still performance. Moreover, specific climatic conditions, such as those in Baghdad, have not been thoroughly considered in previous research, leading to a gap in tailored design recommendations that optimize distillate productivity for different environments. Addressing these gaps through an integrated multi-software approach and focusing on specific regional climates can significantly advance the efficiency and applicability of solar desalination technologies.

This research aims to significantly enhance water desalination efficiency in solar stills by optimizing the glass cover tilt angle, leveraging comprehensive data analysis through MATLAB programming. Despite previous advancements in solar distillation, there remains a critical gap in understanding the optimal design configurations tailored to specific climatic conditions, such as those in Baghdad. This study addresses this gap by meticulously analyzing the impact of varying tilt angles on distillation productivity, utilizing an integrated approach that combines SOLIDWORKS modelling, ANSYS CFD simulations, and MATLAB algorithms. By employing this multi-software methodology, we aim to provide a robust, empirically validated design recommendation that significantly advances the field of solar water desalination, delivering a practical solution to water scarcity challenges in arid regions.

## 2. Methodology

The methodology section of the paper focuses on analyzing a single-slope solar still, specifically designed for Baghdad's climatic conditions. The section begins by presenting theoretical equations essential for the solar still's design and operation, including aspects of Computational Fluid Dynamics (CFD) and heat transfer. Utilizing SOLIDWORKS, the solar still is designed, followed by simulations in ANSYS Fluent and MATLAB. These simulations are critical in evaluating the still's performance at 25, 30, 32.5, 35, and 40 degrees to determine the most efficient angle for water distillation in Baghdad.

### *2.1 Aerodynamic Science and Its Equations*

Computational Fluid Dynamics (CFD), a branch of fluid mechanics, employs numerical methods and computational algorithms to simulate and analyze fluid flow behaviors [14]. Fundamental to CFD are the Navier-Stokes equations, which describe fluid motion through conservation of momentum, mass, and energy [15] Key equations used include [16]:

#### *2.1.1 Continuity equation*

Bernoulli's equation links pressure, velocity, and height in fluid flow without friction. It's a key equation in fluid mechanics, first described by Daniel Bernoulli in 1738 and later fully formulated by Leonhard Euler in 1755. It assumes uniform properties across a fluid's cross-section in a tube-shaped area. The equation is [17]:

$$\frac{\partial \rho}{\partial t} + \operatorname{div}(\rho u) = 0 \tag{1}$$

### *2.1.2 Momentum equation*

The momentum equation accounts for the conservation of momentum and reflects the relationship between forces and acceleration within a fluid. It is given by [17]:

$$\frac{\partial(\rho u)}{\partial t} + div(\rho u\mathrm{u}) = -\frac{\partial p}{\partial x} + div(\mu \times \mathrm{grad}u) + S_{Mx} \quad \text{(x – direction)} \tag{2}$$

$$\frac{\partial(\rho v)}{\partial t} + div(\rho v\mathrm{u}) = -\frac{\partial p}{\partial y} + div(\mu \times \mathrm{grad}v) + S_{My} \quad \text{(y – direction)} \tag{3}$$

$$\frac{\partial(\rho w)}{\partial t} + div(\rho w\mathrm{u}) = -\frac{\partial p}{\partial z} + div(\mu \times \mathrm{grad}w) + S_{Mz} \quad \text{(z – direction)} \tag{4}$$

### *2.1.3 Energy equation*

$$\frac{\partial(\rho i)}{\partial t} + div(\rho i\mathrm{u}) = -pdiv(\mathrm{u}) + div(k \times \mathrm{grad}T) + \Phi + S_i \tag{5}$$

### *2.2 Heat Transfer*

Heat transfer involves the flow of thermal energy resulting from temperature differences in an area [18].

### *2.2.1 Conduction*

This involves the direct transfer of heat through a material without the material itself moving. It's governed by Fourier's Law, expressed as [18]:

$$q = -kA\frac{\Delta T}{\Delta x} \tag{6}$$

In the context of heat transfer, q represents the rate of heat transfer measured in Watts (W), k stands for the thermal conductivity of the material, denoted in Watts per meter Kelvin, A refers to the cross-sectional area in square meters ($m^2$), ΔT is the temperature difference across the material, measured in Kelvin (K) or degrees Celsius (°C), and Δx signifies the thickness of the material in meters (m).

### *2.2.2 Conduction*

This mode describes heat transfer between a solid surface and a fluid, or between fluids, due to fluid motion. Newton's Law of Cooling is used to describe it, shown as [18]:

$$q = hA(T_s - T_\infty) \tag{7}$$

In the context of convection heat transfer, h represents the convective heat transfer coefficient, measured in Watts per square meter Kelvin ($\frac{w}{m^2.K}$). A denotes the surface area in square meters ($m^2$), $T_s$ is the surface temperature, which can be in Kelvin (K) or degrees Celsius (°C), and $T_\infty$ refers to the fluid temperature, also measured in Kelvin or degrees Celsius.

### *2.2.3 Radiation*

This is heat transfer in electromagnetic waves, not requiring a medium. The Stefan-Boltzmann Law, is used for its description as shown [18]:

$$q = \epsilon\sigma A({T_1}^4 - {T_2}^4) \tag{8}$$

In radiation heat transfer, ϵ signifies the emissivity of the material, ranging between 0 and 1. σ represents the Stefan-Boltzmann constant, valued at $5.67 \times 10^8 \ \frac{W}{m^2.K^4}$. A refers to the surface area, measured in square meters ($m^2$). $T_1$ and $T_2$ are the absolute temperatures of the two surfaces involved, measured in Kelvin (K).

### *2.3 Theoretical Background Used in Solar Still*

All equations used below is dependent on these references [19,20] with small changes in some symbols.

### *2.3.1 Solar incidence angle calculation*

$$\theta i = arccos(sin(\alpha) \cdot cos(\beta) + cos(\alpha) \cdot sin(\beta) \cdot cos(\psi_{adjusted})) \tag{9}$$

The Angle of Solar Incidence ($\theta i$) measures the deviation of incoming solar rays from a surface's perpendicular line, ranging from 0° (direct hit) to 90° (parallel). The Solar Elevation Angle (α) denotes the sun's relative position to the horizon, being 90° when directly overhead and 0° at sunrise and sunset. The Slope Angle (β) refers to the inclination of surfaces like solar collectors, from 0° (horizontal) to 90° (vertical). The Adjusted Solar Azimuth Angle (adjusted ψ adjusted ) calculates the sun's position about cardinal directions, factoring in orientation adjustments for computational accuracy.

### *2.3.2 Solar radiation calculation*

$$Solar\ radiation = solar\ constant \times sola\ efficiency \times sin(180\pi \times \alpha) \times cos(\theta i) \tag{10}$$

### *2.3.3 Temperature Variation ($T_v$)*

$$T_v = \frac{Tmax - Tmin}{2} \times \sin\left(\frac{\pi \times (time - midday)}{Tmax - Tmin}\right) + \frac{Tmax + Tmin}{2} \tag{11}$$

### *2.3.4 Heat transfer calculation*

$$Heat\ gain\ glass = solar\_radiation \times glass\ transmittance \tag{12}$$

$$Heat\ loss\ conv = h_{\ conv\ turbulent} \times water\ area \times \Delta T_{\ conv} \tag{13}$$

$$Net\ heat\ gain = heat\ gain\ glass - \ heat\ loss\ conv \tag{14}$$

### *2.3.5 Evaporation rate calculation*

$$Evaporation\ Rate = \frac{net\ heat\ gain \times water\ area}{latent\ heat} \quad (15)$$

### *2.4 Single-Slope Solar Still Design and Analysis*

In this part of the paper, the work begins, focusing on the design and analysis of a single-slope solar still for Baghdad. The SOLIDWORKS design process incorporates specific dimensions and angles to explore optimal efficiency. The section outlines the crucial parameters and settings used in the simulations with ANSYS Workbench and MATLAB, highlighting the detailed approach taken for computational analysis. This foundation sets the stage for a comprehensive evaluation of the solar still's performance under various conditions, aiming to identify the most effective angle for maximum efficiency. Figure 1 below shows single slope soler still and its dimensions.

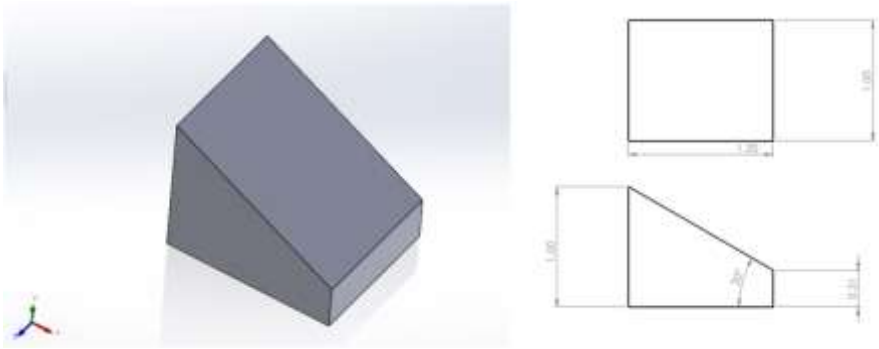

**Fig. 1.** Single Slope Soler still and its dimensions design by SOLIDWORKS

In the above drawing, the inclination of the glass cover is 30, but as it is known, there are 4 other angles which are 25,32,35.5 and 40, but they are all the same principle because the length, width and depth are the same. The simulation was configured to model the solar still performance over the working duration of 9 am to 5 pm. This hourly time range was utilized across the software suite encompassing ANSYS Workbench and MATLAB to execute the simulations and extract the resultant distillate output data, enabling comparison between the angles to determine the optimum tilt. After constructing the still geometry within the SOLIDWORKS CAD environment and finalizing the design, the model was imported into ANSYS Workbench for physics simulations. Mesh generation was undertaken through built-in finite element-based algorithms to discretize the still body into fine elements to bolster computational accuracy. A normal meshing approach was adopted with 3 mm global edge sizing. The mesh metrics including skewness ratio, orthogonality and aspect ratio were analyzed to verify mesh quality for CFD calculations. The mesh elements and nodal coordinates data were then transferred to simulation module for further processing. Figure 2 shows mesh results of single slope solar still and named Selections for boundary condition of solar still.

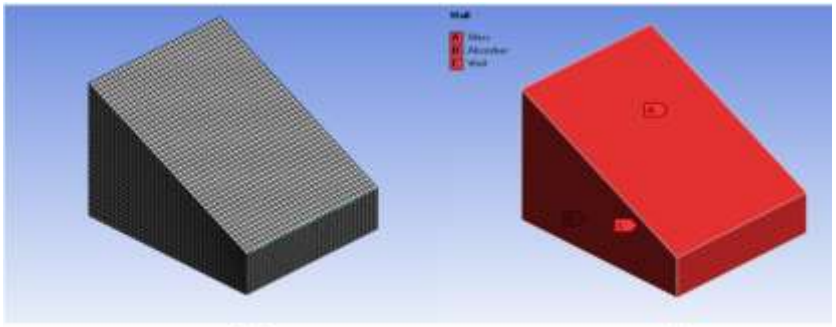


**Fig. 2.** (a) Mesh results of single slope solar still; (b) Named Selections for boundary condition of solar still

Figure 3 below shows the skewness values.

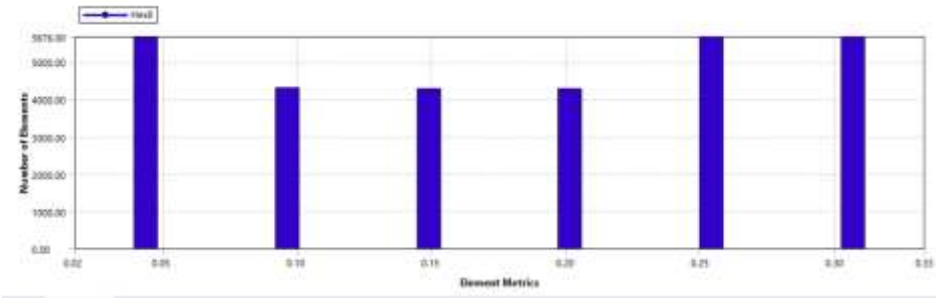

**Fig. 3.** The Skewness values of mesh quality

The table below presents the key input data for the MATLAB simulation code. It encompasses the critical design and operational attributes of the single slope solar still, collated from relevant literature. These inputs will be fed into the model to replicate the system conditions and output performance accurately. Table 1 below shows the data selected for this project depending on location and design requirements.

**Table 1**
Shows the data that selected for this project depends on location and design requirements [21-23]

| Parameter | Value |
|---|---|
| Latitude | 33.312805 |
| Glass transmittance | 0.9 |
| Glass thickness | 1.5 cm |
| Wall thickness | 2 cm |
| Specific heat for wall | 2400 J/kgKfor wood |
| Density of wall | 600 $kg/m^3$ for wood |
| Absorber thickness | 2 mm |
| Density of absorber | 8960 $kg/m^3$ for copper |
| Specific heat for absorber | 385 J/kgK for copper |
| Tmax , Tmin | $46^{\circ}$ , $26^{\circ}$ |
| Specific heat for glass | 840 J/kgK |
| Density of cover glass | 2500 $kg/m^3$ |
| Laten heat for water | $2.266 \times 10^6$ J/kg |

The above settings will be used in the simulation process. The heat equations that were previously explained will be relied upon in writing. In the next section, the results of the simulation on ANSYS will be reviewed, as well as the results resulting from the simulation on MATLAB, and a comparison will be made between all angles to find out the optimal angle.

## 3. Results

The outcomes obtained from the numerical simulations are presented and analyzed in the results section. First, the Computational Fluid Dynamics (CFD) analysis results are discussed using ANSYS Fluent software. Then, a detailed examination of the numerical analysis results obtained using MATLAB is provided, along with comments and observations on these findings. The insights drawn from both analyses are combined to offer a comprehensive understanding of the solar still's performance at different glass cover tilt angles, enabling the determination of the optimal angle for achieving the highest distillate productivity under Baghdad's climatic conditions. The presented results are supported by quantitative data and illustrative graphs, leading to clear and actionable conclusions regarding enhancing water desalination efficiency in solar stills.

### *3.1 ANSYS Fluent Results*

ANSYS Fluent was used to determine some results related to pressure contours, Density, and some other factors such as water volume fraction and vapor fraction. The figures below clarify that. Figures 4 and 5 below show the Ansys fluent analysis results for pressure, density and volume fractions.

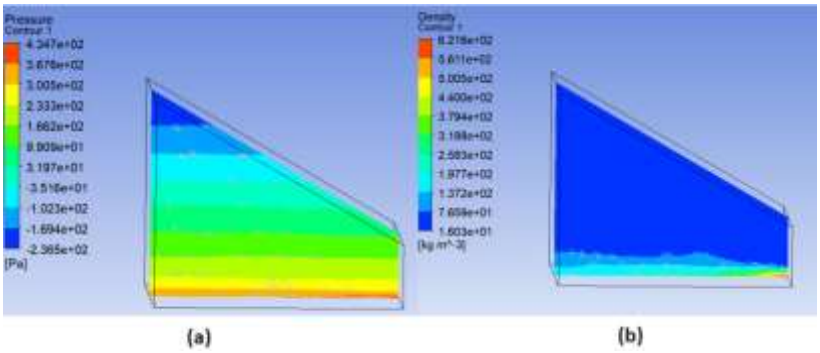


**Fig. 4.** (a) Pressure contours of solar still. (b) Density contours of solar still

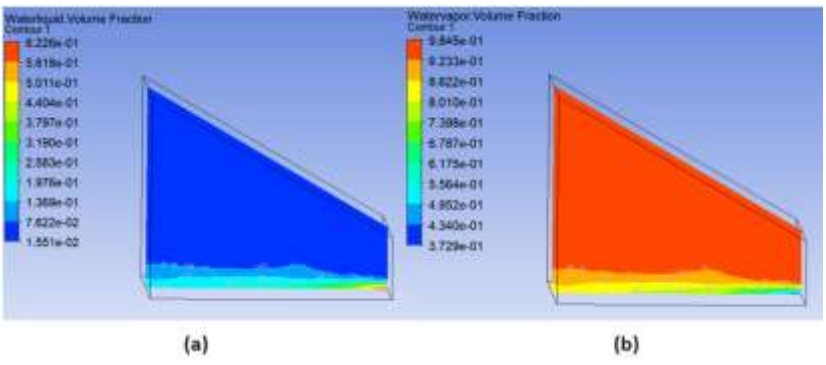


**Fig. 5.** (a) Volume fraction of water liquid in solar still; (b) Volume fraction of water vapor in solar still

### *3.2 MATLAB Analysis Results*

Figure 6 below shows the Distilled water volumes along the working day for each angle.

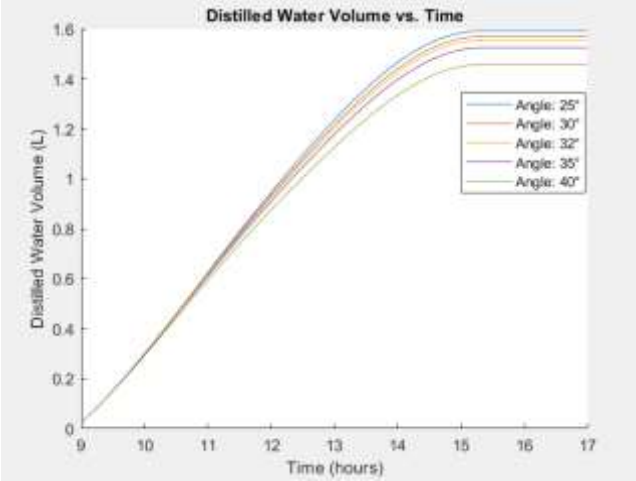


**Fig. 6.** Shows the Distilled water volumes along the working day for each angle

Table 2 below clearly shows the amount of water in litter produced at the end of each hour and at the end of the day.

**Table 2**
The values of desalted water in litters against time for each angle during the day

| | Cover surface slope | | | | |
|---|---|---|---|---|---|
| Time (hour) | θ=25° | θ=30° | θ=32° | θ=35° | θ=40° |
| 9.00 | 0.02296 | 0.02324 | 0.02327 | 0.02324 | 0.02298 |
| 10.00 | 0.29877 | 0.30027 | 0.2999 | 0.29833 | 0.29297 |
| 11.00 | 0.62329 | 0.62076 | 0.61775 | 0.61109 | 0.59434 |
| 12.00 | 0.94486 | 0.93257 | 0.92457 | 0.90927 | 0.87512 |
| 13.00 | 1.23552 | 1.21387 | 1.20103 | 1.17734 | 1.12621 |
| 14.00 | 1.46559 | 1.44055 | 1.42532 | 1.39695 | 1.33513 |
| 15.00 | 1.58476 | 1.56129 | 1.54582 | 1.51617 | 1.44975 |
| 16.00 | 1.59231 | 1.56973 | 1.55442 | 1.52476 | 1.45773 |
| 17.00 | 1.59231 | 1.56973 | 1.55442 | 1.52476 | 1.45773 |
| Unit | | | L | | |

The evaporation rate is shown in the figure 7 below, as well as the table 3 below the figure. As can be seen, the evaporation rate peaks at 12 mm, which is the highest temperature during the day.

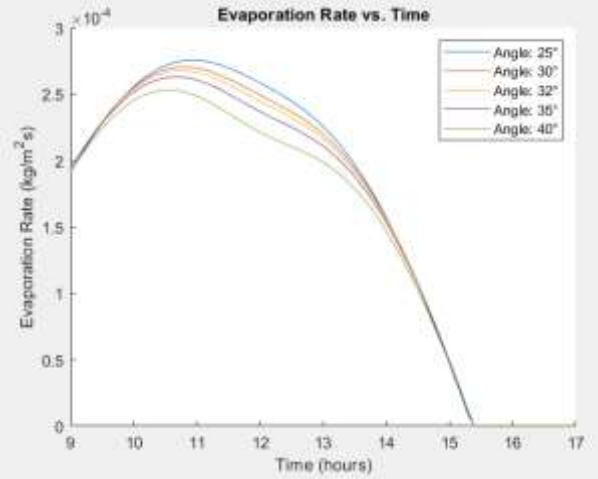


**Fig. 7.** Shows the evaporation rate along the working day for each angle

**Table 3**
The evaporation rate for each angle from 9.00 am to 17.00 pm

| | Cover surface slope | | | | |
|---|---|---|---|---|---|
| Time (hour) | θ=25° | θ=30° | θ=32° | θ=35° | θ=40° |
| 9.00 | 0.000191 | 0.000194 | 0.000194 | 0.000194 | 0.000192 |
| 10.00 | 0.000256 | 0.000255 | 0.000254 | 0.000252 | 0.000245 |
| 11.00 | 0.000276 | 0.000270 | 0.000266 | 0.000261 | 0.000249 |
| 12.00 | 0.000259 | 0.000249 | 0.000245 | 0.000237 | 0.000221 |
| 13.00 | 0.000226 | 0.000220 | 0.000217 | 0.000211 | 0.000199 |
| 14.00 | 0.000157 | 0.000157 | 0.000156 | 0.000153 | 0.000147 |
| 15.00 | 0.000047 | 0.000049 | 0.000049 | 0.000049 | 0.000047 |
| 16.00 | 0 | 0 | 0 | 0 | 0 |
| 17.00 | 0 | 0 | 0 | 0 | 0 |
| Unit | | | $kg/m^2.s$ | | |

Figure 8 and table 4 below show the amount of water remaining from its original height at the end of the work.

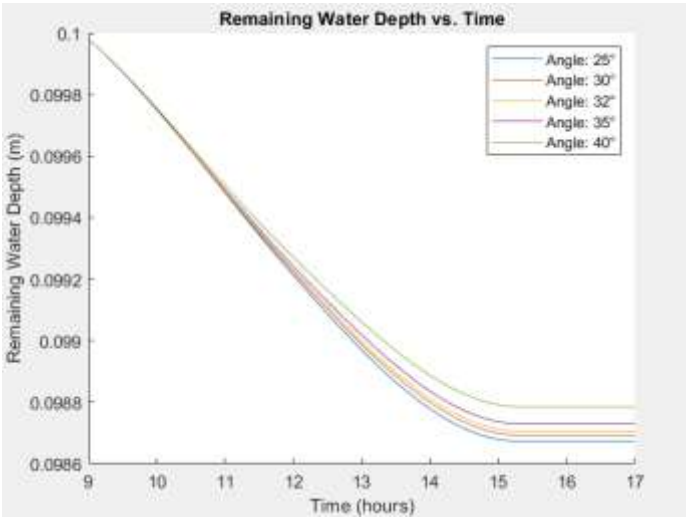


**Fig. 8.** Shows the remaining water depth at each hour for each angle

**Table 4**
The Remaining water depth for each angle from 9.00 am to 17.00 pm

| | Cover surface slope | | | | |
|---|---|---|---|---|---|
| Time (hour) | θ=25° | θ=30° | θ=32° | θ=35° | θ=40° |
| 9.00 | 0.09998 | 0.09998 | 0.09998 | 0.09998 | 0.09998 |
| 10.00 | 0.09975 | 0.09975 | 0.09975 | 0.09975 | 0.09976 |
| 11.00 | 0.09948 | 0.09948 | 0.09949 | 0.09949 | 0.09950 |
| 12.00 | 0.09921 | 0.09922 | 0.09923 | 0.09924 | 0.09927 |
| 13.00 | 0.09897 | 0.09899 | 0.09900 | 0.09902 | 0.09906 |
| 14.00 | 0.09878 | 0.09880 | 0.09881 | 0.09884 | 0.09889 |
| 15.00 | 0.09868 | 0.09870 | 0.09871 | 0.09874 | 0.09879 |
| 16.00 | 0.09867 | 0.09869 | 0.09870 | 0.09873 | 0.09879 |
| 17.00 | 0.09867 | 0.09869 | 0.09870 | 0.09873 | 0.09879 |
| Unit | | | mm | | |

The temperature of the absorber, which is the lower wall made of copper for all angles, is constant, as in the figure 9 below, because the material has not changed.

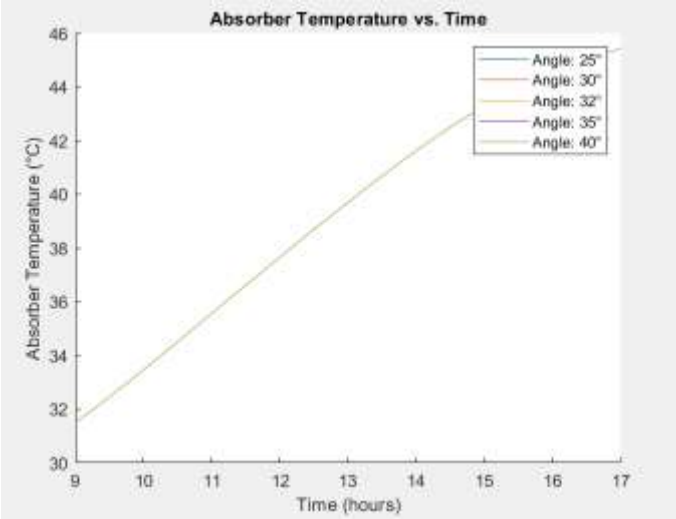


**Fig. 9.** Shows the basin or absorber temperatures at each hour for each angle

Table 5 below shows the Values of absorber temperatures for each angle from 9.00 am to 17.00 pm.

**Table 5**
Values of absorber temperatures for each angle from 9.00 am to 17.00 pm

| | Cover surface slope | | | | |
|---|---|---|---|---|---|
| Time (hour) | θ=25° | θ=30° | θ=32° | θ=35° | θ=40° |
| 9.00 | 31.5123178 | 31.5129533 | 31.5130351 | 31.5129727 | 31.512376 |
| 10.00 | 32.9796086 | 32.9794602 | 32.9791789 | 32.9785201 | 32.9767955 |
| 11.00 | 34.5108632 | 34.509274 | 34.5083931 | 34.5068123 | 34.5034968 |
| 12.00 | 36.0705703 | 36.0680601 | 36.0668078 | 36.0646679 | 36.0604195 |
| 13.00 | 37.6259479 | 37.6243587 | 37.6234779 | 37.621897 | 37.6185815 |
| 14.00 | 39.1330743 | 39.1329259 | 39.1326447 | 39.1319859 | 39.1302613 |
| 15.00 | 40.5526458 | 40.5532813 | 40.5533631 | 40.5533007 | 40.5527039 |
| 16.00 | 41.8544618 | 41.8550578 | 41.8551885 | 41.8552687 | 41.8550929 |
| 17.00 | 43.0143084 | 43.0144447 | 43.0144525 | 43.014414 | 43.0142165 |
| Unit | | | °C | | |

For glass temperature also the Temperatures are the same for all angles in the same reason of the absorber wall above, which is the material is the same and will not change.

Figure 10 below shows glass cover temperatures at each hour for each angle.

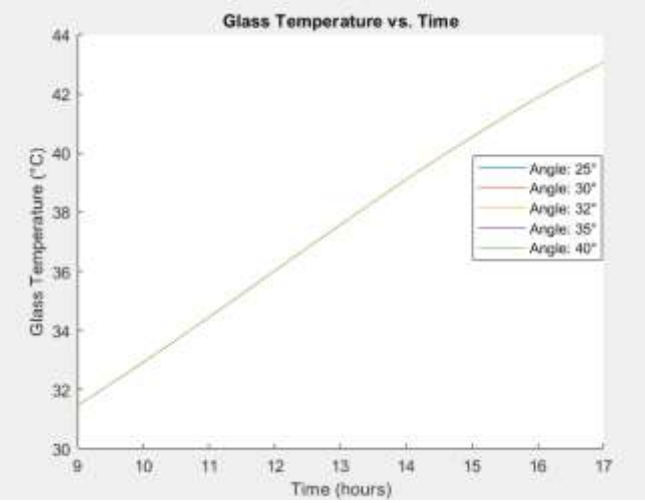


**Fig. 10.** Shows the glass cover temperatures at each hour for each angle

Table 6 below shows values of glass cover temperatures for each angle from 9.00 am to 17.00 pm.

**Table 6**
Values of glass cover temperatures for each angle from 9.00 am to 17.00 pm

| | Cover surface slope | | | | |
|---|---|---|---|---|---|
| Time (hour) | θ=25° | θ=30° | θ=32° | θ=35° | θ=40° |
| 9.00 | 31.4715 | 31.4717 | 31.4717 | 31.4717 | 31.4715 |
| 10.00 | 32.9251 | 32.9251 | 32.925 | 32.9249 | 32.9245 |
| 11.00 | 34.4521 | 34.4518 | 34.4516 | 34.4512 | 34.4505 |
| 12.00 | 36.0155 | 36.0149 | 36.0146 | 36.0142 | 36.0132 |
| 13.00 | 37.5778 | 37.5775 | 37.5773 | 37.5769 | 37.5762 |
| 14.00 | 39.0996 | 39.0995 | 39.0995 | 39.0993 | 39.099 |
| 15.00 | 40.5427 | 40.5428 | 40.5429 | 40.5428 | 40.5427 |
| 16.00 | 41.8727 | 41.8729 | 41.8729 | 41.8729 | 41.8729 |
| 17.00 | 43.0586 | 43.0587 | 43.0587 | 43.0587 | 43.0586 |
| Unit | | | °C | | |

Regarding the value of solar radiation, the figure 11 and table 7 below show its value at different temperatures. As can be seen, its highest value is associated with the highest temperature during the day, that is, at 12 noon.

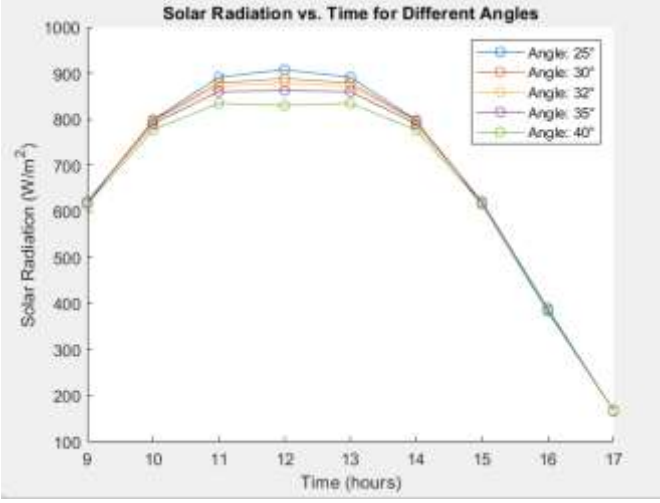


**Fig. 11.** Shows the solar radiation values at each hour on the incline surface at each angle

**Table 7**
Solar Radiation values on the incline surface at each angle from 9.00 am to 17.00 pm

| | Cover surface slope | | | | |
|---|---|---|---|---|---|
| Time (hour) | θ=25° | θ=30° | θ=32° | θ=35° | θ=40° |
| 9.00 | 616.1107 | 616.1107 | 616.1107 | 616.1107 | 616.1107 |
| 10.00 | 777.0035 | 777.0035 | 777.0035 | 777.0035 | 777.0035 |
| 11.00 | 834.5790 | 834.5790 | 834.5790 | 834.5790 | 834.5790 |
| 12.00 | 829.8294 | 829.8294 | 829.8294 | 829.8294 | 829.8294 |
| 13.00 | 834.5790 | 834.5790 | 834.5790 | 834.5790 | 834.5790 |
| 14.00 | 777.0035 | 777.0035 | 777.0035 | 777.0035 | 777.0035 |
| 15.00 | 616.1107 | 616.1107 | 616.1107 | 616.1107 | 616.1107 |
| 16.00 | 388.1248 | 388.1248 | 388.1248 | 388.1248 | 388.1248 |
| 17.00 | 166.5593 | 166.5593 | 166.5593 | 166.5593 | 166.5593 |
| Unit | | | $W/m^2$ | | |

After a thorough analysis and comparative analysis of the simulation outcomes across the range of cover tilt configurations, it has been demonstrated that 25° represents the optimal angle in alignment with maximized distillate productivity in the city of Baghdad on July 25th from 9 am to 5 pm. This deduction has been driven by the definitive trend of superior performance metrics at 25° inclination under the ambient conditions and weather constraints constitutive of Baghdad during the chosen timeline. In particular, the hourly computations and final distillate volumes detect 1.58- and 1.59-liters production at 25° tilt corresponding to the end of operational timeframe and across the designated 9 am to 5 pm working duration. In contrast, the total distillates at other measured angles of 30°, 32°, 35° and 40° amount to 1.56, 1.55, 1.52 and 1.45 liters respectively. Thus, a 3.3% enhanced productivity is attained at 25° in Baghdad on July 25th, indicative of its advantageous orientation for heightened incident irradiation and evaporation rates under the region's summer climatic conditions. The improved light interception lowering reflective losses combined with an effective balance between absorbing adequate thermal energy while minimizing convective heat dissipation to the hot ambient surroundings plays a pivotal role. Furthermore, the MATLAB plots demonstrate superior evaporation rates, glass temperature profiles and solar irradiation influxes at 25° tilt in Baghdad verifying congruent trend across outcomes reinforcing the trimmed angle as optimal for water distillation systems intended for local deployment.

## 4. Conclusions

This study successfully identifies the optimal angle for solar distillation in Baghdad, discovering that a 25° inclination maximizes water desalination. This finding emerges from a detailed analysis using various software tools, underscoring the importance of a multifaceted approach in research. The integration of different analytical methods has not only enhanced the accuracy of the results but also exemplifies cost-effective alternatives to physical testing. This research offers significant insights for future applications, providing a practical and efficient blueprint for designing solar distillation systems in various climatic conditions. The methodology and findings have broader implications, potentially aiding global efforts toward sustainable water and energy solutions.

## Acknowledgement
This research was fully funded by Altinbas University.

## References
[1] H. T. El-Dessouky and H. M. Ettouney, Fundamentals of Salt Water Desalination. Amsterdam: Elsevier, 2002. https://doi.org/10.1016/B978-0-444-50810-2.X5000-3
[2] Crittenden, John C., R. Rhodes Trussell, David W. Hand, Kerry J. Howe, and George Tchobanoglous. *MWH's water treatment: principles and design*. John Wiley & Sons, 2012. https://doi.org/10.1002/9781118131473
[3] A. Vogelpohl, Distillation: The Theory, 2nd ed. De Gruyter. 2021. https://doi.org/10.1515/9783110333466
[4] Bhasker, S. S., E. Sathwik Reddy, S. Abhishek, S. Murthy, and K. V. Naga Lakshmi. "Optimization & Studies on Extraction of Palma Rosa Oil by Steam Distillation." *Int. J of Eng. Res. & Reviews* 3, no. 3 (2015): 29-34. [Online]. Available: https://www.researchpublish.com/papers/optimization--studies-on-extraction-of-palma-rosa-oil-by-steam-distillation
[5] P. Vishwanath Kumar, A. Kumar, O. Prakash, and A. K. Kaviti, "Solar stills system design: A review," *Renewable and Sustainable Energy Reviews*, vol. 51, pp. 153–181, 2015. https://doi.org/10.1016/j.rser.2015.04.103
[6] Khelifa, A., K. Touafek, H. Ben Moussa, and I. Tabet. "Modeling and detailed study of hybrid photovoltaic thermal (PV/T) solar collector." *Solar Energy* 135 (2016): 169-176. https://doi.org/10.1016/j.solener.2016.05.048
[7] Moh'd A, Al-Nimr, and Khaled S. Qananba. "A solar hybrid system for power generation and water distillation." *Solar Energy* 171 (2018): 92-105. https://doi.org/10.1016/j.solener.2018.06.019
[8] Amiri, Hossein, Mohammad Aminy, Marzieh Lotfi, and Behzad Jafarbeglo. "Energy and exergy analysis of a new solar still composed of parabolic trough collector with built-in solar still." *Renewable Energy* 163 (2021): 465-479. https://doi.org/10.1016/j.renene.2020.09.007
[9] Singh, D. B., J. K. Yadav, V. K. Dwivedi, S. Kumar, G. N. Tiwari, and I. M. Al-Helal. "Experimental studies of active solar still integrated with two hybrid PVT collectors." *Solar Energy* 130 (2016): 207-223. https://doi.org/10.1016/j.solener.2016.02.024
[10] Jasim, Maryam A., Omer K. Ahmed, and Yaser Alaiwi. "Performance of solar stills integrated with PV/Thermal solar collectors: a review." *NTU Journal of Renewable Energy* 4, no. 1 (2023): 97-111. https://doi.org/10.56286/ntujre.v4i1.456
[11] AbdelMeguid, Hossam, and Waleed M. El Awady. "Optimizing solar still performance through glass cover optical properties: A mathematical modeling and theoretical investigation." *Ain Shams Engineering Journal* 15, no. 3 (2024): 102589. https://doi.org/10.1016/j.asej.2023.102589
[12] Nahoui, Azzedine, Redha Rebhi, Giulio Lorenzini, and Younes Menni. "Numerical study of a basin type solar still with a double glass cover under winter conditions." *Journal of Advanced Research in Fluid Mechanics and Thermal Sciences* 88, no. 1 (2021): 35-48. https://doi.org/10.37934/arfmts.88.1.3548
[13] Haddad, Zakaria, Abla Chaker, Azzedine Nahoui, Mohamed Salmi, and Islam Laifa. "Experimental Study of an Inclined Wick Solar Still Operating in Drop by Drop System Under The Climatic Conditions of Hodna's Region, Algeria." *Journal of Advanced Research in Fluid Mechanics and Thermal Sciences* 94, no. 1 (2022): 188-199. https://doi.org/10.37934/arfmts.94.1.188199
[14] Anderson, John David, and John Wendt. *Computational fluid dynamics*. Vol. 206. New York: McGraw-hill, 1995. https://doi.org/10.1136/bmj.332.7555.1456-a
[15] F. J.H., P. M., and R. L. Street, Computational Methods for Fluid Dynamics, 4th ed. Gewerbestrasse: Springer Nature Switzerland AG, 2020. https://doi.org/10.1007/978-3-319-99693-6

[16] Versteeg, Henk Kaarle. *An introduction to computational fluid dynamics the finite volume method, 2/E*. Pearson Education India, 2007.
[17] F. White and H. Xue, FLUID MECHANICS, 9th ed. New York: McGraw-Hill, 2021. [Online]. Available: https://www.mheducation.com/highered/product/fluid-mechanics-white-xue/M9781260258318.html
[18] T. L. Bergman and A. S. Lavine, Fundamentals of Heat and Mass Transfer, 8th ed. New York: Wiley & Sons, Inc., 2017. [Online]. Available: https://www.wiley.com/en-us/Fundamentals+of+Heat+and+Mass+Transfer%2C+8th+Edition-p-9781119353881
[19] Duffie, John A., William A. Beckman, and Nathan Blair. *Solar engineering of thermal processes, photovoltaics and wind*. John Wiley & Sons, 2020.
[20] L. Łabędzki, EVAPOTRANSPIRATION, 1st ed. Rijeka, 2011. https://doi.org/10.5772/585
[21] Yin, Shuo, Xiao-fang Wang, Wen-ya Li, and Bao-peng Xu. "Numerical investigation on effects of interactions between particles on coating formation in cold spraying." *Journal of thermal spray technology* 18 (2009): 686-693. https://doi.org/10.1007/s11666-009-9390-6
[22] Munsch, Marie, Nicolas Bourdet, Caroline Deck, and Rémy Willinger. "Lateral glazing characterization under head impact: experimental and numerical investigation." In *21st International Technical Conference on The Enhanced Safety of Vehicles (in Germany), Stuttgart*. 2009.
[23] Karol, Sikora, Hao Jianli, Galobardes Isaac, Xing Weiqi, Wei Subo, and Chen Zitong. "Feasibility study on further utilization of timber in China." In *IOP Conference Series: Materials Science and Engineering*, vol. 383, no. 1, p. 012029. IOP Publishing, 2018. https://doi.org/10.1088/1757-899X/383/1/012029